Indian Journal of Chemistry
Vol. 61, July 2022, pp. 771-775

The application value of a new Zn(II) coordination polymer in the early diagnosis and treatment of infantile rickets

Xiaoqian Lv*, Na Liu & Zhanru Yin
Hengshui People's Hospital, Hengshui, Hebei, China
E-mail: okj460579@163.com

Received 16 January 2022; accepted (revised) 10 May 2022

In the present study, a new 1D Zn(II) coordination polymer (CP) on the basis of 2,5-bis(pyridine-2-yl)-1,3,4-thiadiazole (L) as linking ligand with the chemical formula of $[ZnLCl_2]_n$ has been created *via* blending L with Zn salt ($ZnCl_2$) and studied through single crystal X-ray diffraction and elemental analysis. Its application values on the early diagnosis and treatment of infantile rickets were determined and the relevant mechanism was studied in the meanwhile. Then, the QCT was used to measure the bone density of the infantile rickets animal after adding compound. Moreover, the activity of the wnt signaling routine in the bone tissue was assessed *via* real time RT-PCR. By investigating into the detail of the binding conformation from a molecular level, molecular docking simulation reveals that the expected biological activity of the Zn complex comes from the pyridine group.

Keywords: Coordination polymer, infantile rickets, molecular docking

Infantile rickets is rickets associated with vitamin D deficiency. Infantile rickets are generally caused by perinatal or postnatal vitamin D deficiency, calcium and phosphorus metabolism disorders and other factors caused by abnormal bone development and mental system diseases[1,2]. Thus, new candidates should be developed for the treatment of infantile rickets.

In recent decades, many experiments have proved that CPs plays a great role in the medical field. It can be used to inhibit bacteria and fungi, inhibit the activity of cancer cells, catalyze some chemical reactions and treat a variety of diseases[3-6]. Because N atoms exist widely in natural substances and drugs, scientists have been studying the creation of CPs containing nitrogen atoms and chelating ligands[7-10]. The results of many experiments show that the coordination between organic molecules and metals has high efficiency. At present, 1,3,4-thiadiazole derivatives, for instances, 2,5-bis(pyridin-2-yl)-1,3,4-thiadiazole (L), have been proved to be effective, and on this basis, single metal complexes and multi metal complexes have been formed. The bioactivity test results of the complexes show that the ligand combination efficiency is positively correlated with the metal coordination environment[11-13]. On the other hand, although zinc is not strictly a transition metal, but it shares many bioinorganic properties with the transition metals due to the particular properties of its coordination compounds. As a borderline Lewis acid zinc is a component of so many metalloenzymes and has a specific role in the bioinorganic processes of these enzymes[14]. Therefore, it is the second most abundant element in the 3d transition metals after iron in the human body. Unlike iron and copper that have different oxidation states, Zn (II) ion plays only a structural role in forming appropriate enzymes by means of coordination to amino acids such as cysteine and histidine in approximately tetrahedral coordination geometry. Its d10 configuration and zero ligand field stabilization energy give it a potential to adopt four, five, or six – coordination, without a marked preference for six coordination, when a zinc enzyme interacts with a substrate[15]. In order to design and synthesize model compounds of the zinc enzymes, many coordination chemistry researchers have focused their work on the synthesis of Zn (II) complexes with nitrogen, oxygen, and sulfur donor ligands which can mimic the active site of these enzymes. Zinc is the only metal ion that can facilitate the rewinding of DNA. Additionally, many zinc complexes have shown anticonvulsant, antidiabetic, anti-inflammatory, antimicrobial, antioxidant, and anticancer properties and some of them have also been tested for the treatment of Alzheimer's disease[16-18]. In the present study, a new 1D Zn(II) coordination polymer (CP) on the basis of 2,5-bis(pyridine-2-yl)-1,3,4-thiadiazole (L) as linking ligand with the chemical formula of $[ZnLCl_2]_n$ has been created *via* blending L with Zn salt ($ZnCl_2$) and studied

through single crystal X-ray diffraction and elemental analysis. Several medical research were accomplished in this study to measure the application values of the fresh compound on the treatment of infantile rickets, the mechanism of the new compound was explored at the same time. Molecular docking simulation is a widely used and popular technic for sampling the binding conformation and therefore confirms the detailed binding interactions from the molecular level. Hence, the molecular docking simulation has been adopted in the current work to study the binding interactions from potential binding poses.

Experimental Section

All experimental materials were purchased from the manufacturer. If there are no special requirements, no additional treatment was required. The infrared (IR) spectra were implemented (ranging from 400 to 4000 cm^{-1}) through the Nicolet Impact 410 FTIR spectrometer utilizing KBr pellets. Elemental analyses (Carbon, hydrogen, nitrogen) were operated on the Perkin Elmer 2400 analyzer.

Preparation and characterization for $[ZnLCl_2]_n$, 1

0.1 mmol L dissolved in 5 mL ethanol in the environment of 0.2 mmol $ZnCl_2$ aqueous solution with magnetic stirring. After the reaction was carried out for four hours at normal temperature, the solution was filtered and dried in vacuum. After about three weeks, the colorless crystals were aggregated, cleaned with distilled water and dried in vacuum (yield: fifty-two percent). These products are utilized as samples for single crystal X-ray experiments. Anal. calcd. for $C_{12}H_8Cl_2ZnN_4S$. C: 38.28, H: 2.14, N: 14.88, S: 8.51; found: C: 38.35, H: 2.45, N: 14.58, S: 8.41.

X-ray crystallographic determination

Single crystal samples with suitable size, flat shape and smooth surface are installed on the glass fiber for single crystal X-ray structure determination. Reflection data were collected at room temperature on a Bruker AXS SMART APEX II CCD diffractometer with graphite monochrome Mo-Kα radiation (λ = 0.71073 Å). All measured independent reflections ($I > 2\sigma(I)$) were used for structural analysis and semi-empirical absorption correction was performed using the SADABS program. All calculations were performed using OLEX-2[19]. Crystal structures were determined by the direct method. All non-hydrogen atoms are refined by anisotropic refinement using the SHELXL software[20]. The hydrogen atoms of the organic skeleton were fixed in the calculated position, and all non-hydrogen atoms were refined anisotropically and refined by the riding model. Table I exhibits the crystallographic information of compound **1**.

QCT detection

The quantity CT was implemented in the current experiment to determine the bone density of the animal after compound treatment. This experiment was accomplished completely according to the advice with some appropriate changes. Firstly, the fifty BALB/c rats (6-8 weeks, 20-22g) were elected in the current research, which were all obtained from the Model Animal Research Center of Nanjing University (Nanjing, China). The animals were maintained in the environments of forty-five percent humidity and 20–25° C temperature with half the time of light and half the time of darkness every day until the study began. The infantile rickets destroy rats model and the compound was added for cure at the consistence of one, two and five mg/kg. Subsequently, the quantity CT was performed to measure the bone density of the rats after adding compounds. Next, the bone tissue was isolated, and the total RNA in the tissue was extracted *via* TRIZOL reagent.

Real time RT-PCR

The real time RT-PCR was conducted and the activity of the wnt signaling route in the bone tissue after adding compound was measured in the current experiment. After evaluating the consistence of the

Table I — Crystallographic information of compound **1.**

Empirical formula	$C_{12}H_8Cl_2N_4SZn$
Formula weight	376.55
Temperature/K	296.15
Crystal system	monoclinic
Space group	C2/c
a/Å	10.41620(10)
b/Å	12.2263(2)
c/Å	10.9425(5)
α/°	90
β/°	98.2350(10)
γ/°	90
Volume/$Å^3$	1379.18(7)
Z	4
$\rho_{calc}g/cm^3$	1.813
μ/mm^{-1}	2.311
Reflections collected	16359
Independent reflections	1406 [R_{int} = 0.0320, R_{sigma} = 0.0133]
Data/restraints/parameters	1406/0/93
Goodness-of-fit on F^2	1.090
Final R indexes [I>=2σ (I)]	R_1 = 0.0255, ωR_2 = 0.0739
Final R indexes [all data]	R_1 = 0.0281, ωR_2 = 0.0758
Largest diff. peak/hole / e $Å^{-3}$	0.40/-0.20
CCDC	2100737

RNA, the real time RT-PCR was conducted to assess the relative expression of wnt signaling route, using *gapdh* as the internal control.

Simulation details

In the current study, we choose Wnt as the target protein that has been reported to have critical roles in stem cell renewal and in cell fate determination, explicitly, the WntD N-terminal domain-linker has been used, the structure was obtained from protein data bank, the PDB ID is 4KRR[19]. It should be noted that only the amino acid structure of 4KRR is used without existing water molecules and ions. We use AutoDockTools to prepare the grid information on the target protein, for the 4KRR protein, it contains a receptor-binding β hairpin and a large solvent-filled cavity, so the grid box has been placed at the coordinates of 6.679, -28.996 and -13.65 Å, the amount of lattice points in per direction is sixty, the distance between grid points is 0.375 Å. Next, the structure of the Zn complex was generated by Avogadro and optimized by the build-in optimization function. The Zn complex has 2 rotatable dihedrals. 50 binding potential binding poses have been investigated by the Lamarckian Genetic Algorithm. All the molecular docking simulations were accomplished *via* AutoDock 4.2.

Results and Discussion

Structural characterization

Mixing 2,5-bis(pyridine-2-yl)-1,3,4-thiadiazole (L) with $ZnCl_2$ to form the titrated copper complex, $[ZnLCl_2]_n$. The asymmetric part of the one-dimensional Zn(II) CPs studied contains a single molecular formula unit, namely a single Zn^{2+} ion, a single L and double Cl^- counter anions. Complex 1 form the crystal in space group *C* 2/*c* and the complex framework exhibits a neutral one-dimensional infinite alternating chain motif (Figure 1a). Among the complexes, Zn^{2+} ions are at the core and coordinated by four N-atom octahedrons from double bridged bis-chelate heterocyclic ligands in the equatorial position. The chlorine atom is in the axial plane. In practical terms, though Zn^{2+} ions are at the core of the whole structure, the octahedron around Zn^{2+} presents a twisted state. The pyridine rings connected to metallic ions and 1,3,4-thiadiazole are almost coplanar, and the maximum offset in the average plane is 0.330 (2) Å. According to the results of Figure 1b, ligand L links with the nucleus of Zn^{2+} in a cis arrangement to construct a serrated one-dimensional framework, so as to construct an illimitable band running in the [0 0 1] direction. The shortest intra-chain Zn···Zn distance is 5.414 (2) Å, and the shortest inter-chain Zn···Zn distance is 7.928 (2) Å. In the crystallographic framework of **1**, molecules are cross connected by Zn ions to construct illimitable chains in the [0 0] direction. The small H-bond of C–H···Cl determines the cohesion of 1-dimensional polymer framework. While, according to the results of Figure 1c, 1-dimensional chains are combined through π–π stacking inter-reaction and close-contact stacking of 2-pyridyl rings on L to form a 3-dimensional framework. The laminated pyridine ring is parallel to the centroid, and the distances from the centroid to the centroid are 4.019 and 3.991 Å, respectively.

Effect of compound on the bone density of the infantile rickets animal

After the conformation of the fresh compound, its bioactivity was assessed, as there was usually a reduced level of bone density of the infantile rickets animal. So, the QCT was performed and the bone density of the infantile rickets animal was measured and illustrated in Figure 2. According to Figure 2, it is worthy that the level of bone density in the animal group was dramatically declined rather than the control group. After the addition of the fresh compound, the bone density of the infantile rickets animal was up-regulated. The promoting effect of this new compound is closely related to the amount used.

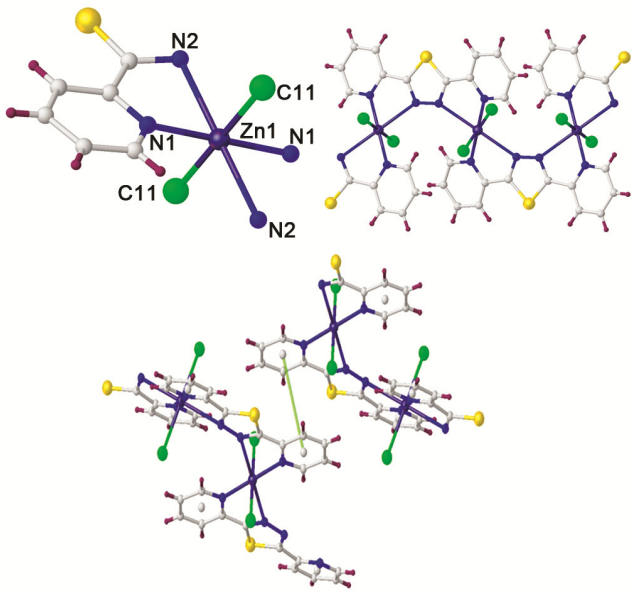

Figure 1 — (a) The coordination surrounding for the Zn(II) ion. (b) The 1-dimensional chain of 1 (c) The π–π stacking interactions in 1

Effect of compound on the wnt signaling pathway in the bone tissue

According to previous experiments, it's proved that the compound played a vital role in increasing the bone density of the infantile rickets animal. As we all know, the wnt signaling route in the bone tissue has a large impact on the infantile rickets. Thus, the real time RT-PCR was then conducted to evaluate the influence of the fresh compound on the activity of wnt signaling route in the bone tissue. The results in Figure 3 described that the activation of wnt signaling route in the control group was higher than the animal group, with P less than 0.005. Under the exposure of the fresh compound, the activity of wnt signaling route in the bone tissue was increased significantly depending on the dosage.

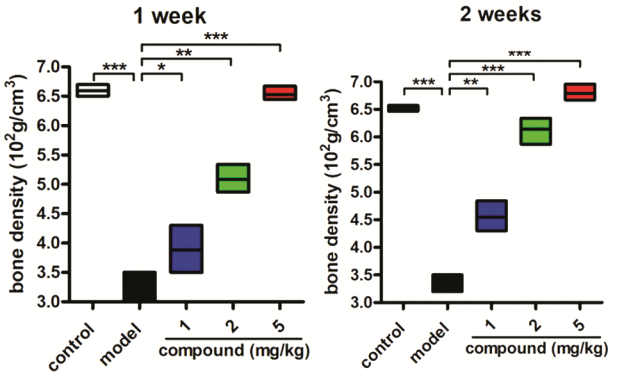

Figure 2 — Significantly increased bone density of the infantile rickets animal after compound treatment. The infantile rickets rats model was established and the compound was added for cure at the consistence of one, two and five mg/kg. The bone density of the infantile rickets animal after adding compound was determined *via* the QCT

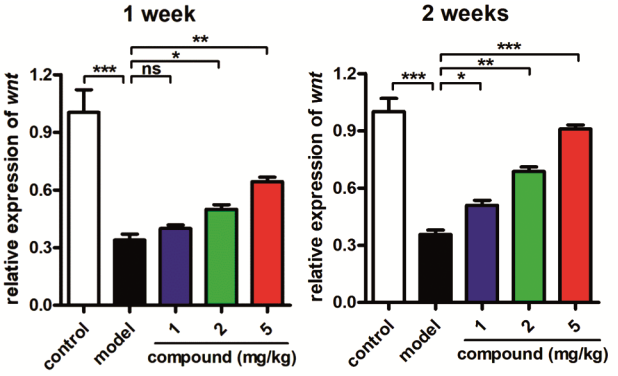

Figure 3 — Obviously active wnt signaling route in the bone tissue after adding compound. The infantile rickets rats model was established and the compound was added for cure at the consistence of one, two and five mg/kg. The real time RT-PCR was implemented and the activity of wnt signaling route in the bone tissue was measured

Molecular docking

The previous experiments illustrated that the Zn complex do have positive activities to the infantile rickets. In order to further understand the fundamental origin of the biological activity, the Wnt protein has been chosen as the target protein since it plays significant role in stem cell renewal and cell fate determination[19]. The structure of the 4KRR contains a receptor-binding β hairpin and a large solvent-filled cavity. Here, we choose the solvent-filled cavity as the docking pocket, since the Zn complex is relatively rigid. 50 potential binding postures were estimated and ranked *via* the Lamarckian Genetic Algorithm, as a tradition and the binding framework with the lowest binding energy were detected.

The binding framework that was chosen from 50 potential binding poses has been displayed in Figure 4. The calculated binding energy is -5.82 kcal/mol, with an estimated inhibition constant of 54.02 μM. It is a good sign that at least an energetically favored binding energy was observed. Further, it is notable that there are two binding interactions formed between the nitrogen atom on the pyridine group and the hydrogen atoms from active residue ARG-156. The lengths for the formed hydrogen bonds are 2.2 and 2.6 Å, respectively. It can be expected that such hydrogen bond lengths could influence the regulation of the protein structure and

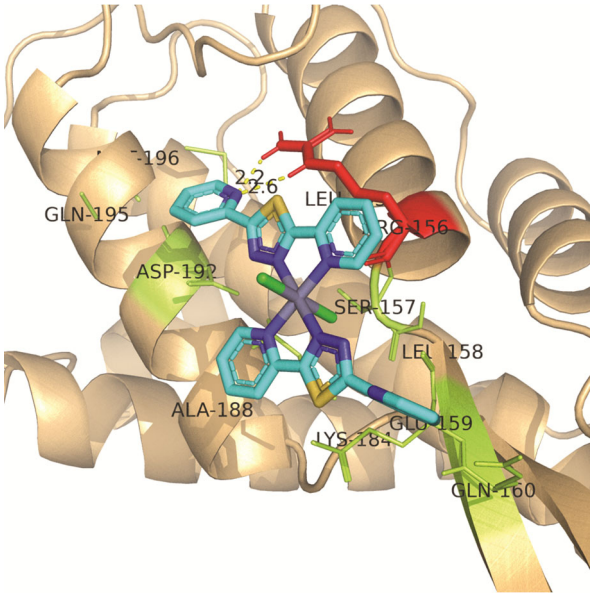

Figure 4 — The binding conformation that was chosen from 50 potential binding poses with the lowest binding energy, the calculated binding energy is –5.82 kcal per mol, and the estimated inhibition coefficient is 54.02 μM. The binding interactions as well as their binding distances are shown explicitly

therefore exhibit the biological activity. Moreover, there are more active residues within the docking pocket, as can be seen, potential binding interactions can be formed with residues ASP-192, GLU-159, LYS-184 and so on. Such results suggest that the Zn complex has excellent biological activity due to its pyridine group.

Conclusion

To sum up we have created a new 1D Zn(II) CP on the basis of 2,5-bis(pyridine-2-yl)-1,3,4-thiadiazole (L) as linking ligand with the chemical formula of $[ZnLCl_2]_n$ has been created *via* blending L with Zn salt ($ZnCl_2$) and studied *via* single crystal X-ray diffraction and elemental analysis. The structural analysis results show that Zn(II) ion sites on the nucleus and depicts coordination framework of slender octahedron. Zn^{2+} ions are coordinated by Four N-atom octahedrons from double ligands in the equatorial position. The chlorine atom is in the axial plane. The results of the results of the QCT showed that bone density of the animal was also up-regulated through the fresh compound by dose-dependently. In addition to this, the compound had a large impact on increasing the activation of the wnt signaling route in the bone tissue in a dose dependent manner. Finally, the conclusion is that the compound has extraordinary application value on infantile rickets by regulating the wnt signaling route in the bone tissue and increasing bone density of the animal. Molecular docking simulation reveals that the expected biological activity of the Zn complex comes from the pyridine group, however, the azathiazole group is not forming any interactions to the active site. Such findings obtained from the molecular level shed light on the novel drug design strategy towards the biological applications.

References

1 Lemoine A, Giabicani E, Lockhart V, Grimprel E & Tounian P, *Arch Pediatr*, 27 (2020) 219.
2 Rusk C, *Neonatal Netw*, 17 (1998) 55.
3 Andreini C & Beritini I, *J Inorg Biochem*, 111 (2012) 150.
4 Kochańczyk T, Drozd A & Krężel A, *Metallomics*, 7 (2015) 244.
5 Huang Y, Zhang S, Chen H, Zhao L, Zhang Z, Cheng P & Chen Y, *Inorg Chem*, 58 (2019) 9916.
6 Beheshti A, Pour M B, Abrahams C T & Motamedi H, *Polyhedron*, 135 (2017) 258.
7 Laitaoja M, Valijakka J & Jänis J, *Inorg Chem*, 52 (2013) 10983.
8 Pathak C, Gupta S K, Gangwar M K, Prakasham A P & Ghosh P, *ACS Omega*, 2 (2017) 4737.
9 Tullius T D, *Metal-DNA Chemistry*, Ed Tullius T D, (American Chemical Society, Washington DC) 1989, pp. 1.
10 Li Q Y, Quan Y, Wei W, Li J, Lu H, Ni R & Wang X J, *Polyhedron*, 99 (2015) 1.
11 Jin C, Zhang S, Zhang Z & Chen Y, *Inorg Chem*, 57 (2018) 2169.
12 Wright A M, Wu Z, Zhang G, Mancuso J L, Comito R J, Day R W, Hendon C H, Miller J T & Dincă M, *Chem*, 4 (2018) 2894.
13 Miller S K, VanDerveer D G & Marzilli L G, *J Am Chem Soc*, 107 (1985) 1048.
14 d'Angelo J, Morgant G, Ghermani N E, Desmaële D, Fraisse B, Bonhomme F, Dichi E, Sghaier M, Li Y, Journaux Y & Sorenson J R J, *Polyhedron*, 27 (2008) 537.
15 Zhou Q, Hambley T W, Kennedy B J, Lay P A, Turner P, Warwick B, Biffin J R & Regtop H L, *Inorg Chem*, 39 (2000) 3742.
16 Tarushi A, Lafazanis K, Kljun J, Turel I, Pantazaki A A, Psomas G & Kessissoglou D P, *J Inorg Biochem*, 121 (2013) 53.
17 Tarushi A, Totta X, Papadopoulos A, Kljun J, Turel I, Kessissoglou D P & Psomas G, *Eur J Med Chem*, 74 (2014) 187.
18 Casas J S, Castellano E E, Couce M D, Ellena J, Sánchez A, Sordo J & Taboada C, *J Inorg Biochem*, 100 (2006) 124.
19 Dolomanov O V, Bourhis L J, Gildea R J, Howard J A K & Puschmann H, *J Appl Crystallogr*, 42 (2009) 339.
20 Sheldrick G M, *Acta Crystallogr Sect C Struct Chem*, 71 (2015) 3.
21 Chu M L H, Ahn V E, Choi H J, Daniels D L, Nusse R & Weis W I, *Structure*, 21 (2013) 1235.